Pergamon

Cement and Concrete Research 31 (2001) 437–441

CEMENT AND CONCRETE RESEARCH

Binary segmentation of aggregate in SEM image analysis of concrete

R. Yang*, N.R. Buenfeld

Department of Civil and Environmental Engineering, Imperial College of Science, Technology and Medicine, Imperial College Road, London SW7 2BU, UK

Received 7 July 2000; accepted 4 December 2000

Abstract

Image analysis of backscattered electron (bse) images has often been used to determine the fraction of the phases in cement paste, such as porosity and anhydrous cement content. However, application of this technique to concrete requires separation of aggregate particles from the paste matrix in the bse image. Binary segmentation of phases is usually based on their grey levels in the image, but the grey levels of aggregate frequently overlap those of the other phases present. In this paper, an algorithm is presented for separating out aggregate particles in the concrete image by a combination of grey-level thresholding, filtering and binary operations. The results demonstrate that the method is able to deal with segmentation of different types of aggregate. © 2001 Elsevier Science Ltd. All rights reserved.

Keywords: SEM; Backscattered electron imaging; Image analysis; Concrete; Aggregate

1. Introduction

Image analysis of backscattered electron (bse) images has often been used to quantify the microstructure of cement pastes, including the determination of porosity [1–5], pore structure [4,6,7], anhydrous cement content [1,2,5] and characterization of the structure of fresh cement paste [8]. In cement paste, anhydrous cement content and porosity can also be determined by techniques such as X-ray diffraction analysis and mercury intrusion porosimetry, respectively. However, these techniques are inappropriate for concrete because their accuracy is greatly reduced by substantial dilution of the cement paste phases due to either the presence of a high proportion of aggregate, if the measurement is based on the whole concrete specimen, or the lack of an effective method for separating the paste from the aggregate if the measurement is based on paste extracted from the concrete.

Image analysis of scanning electron microscopy (SEM) micrographs has previously been shown to have potential for analyzing concrete. Scrivener and Gartner [9] determined porosity profiles in the paste–aggregate transition zone by image analysis. Recently Werner and Lange [10] reported an algorithm that combines conventional grey-level thresholding with a filtering process to differentiate between aggregate particles, cement paste and larger air voids in masonry mortars. Aggregate segmentation from images is essential for determining the porosity and anhydrous cement content of concrete by SEM image analysis. Due to the diluting effect of aggregate, the number of the images required for a statistically acceptable analysis will be impractically large if the measurement is performed without aggregate segmentation. Besides, the high (light) grey levels in some aggregates, resulting from either phases with high backscattering coefficients or poorly polished areas, may overlap with the grey levels of anhydrous cement, affecting quantification of the anhydrous cement content in concrete. Werner's algorithm works on images at low magnification ($50\times$) to determine the area fraction of pores larger than 20 μm. However, to determine the porosity and anhydrous cement content in concrete, a magnification of 400–$1000\times$ is normally chosen. Unfortunately, once an image of such large magnification is involved in analysis, accurate segmentation between the cement paste and the aggregate cannot be easily achieved by grey-level thresholding and filtering alone, particularly for dense concrete.

In the current work, an algorithm is presented for separating aggregate particles in the concrete image at magnifications of up to at least $1000\times$ by combining the techniques of binary operation with those of conventional grey-level thresholding and filtering. This approach can cope with aggregate particles having composite grey levels.

* Tel.: +44-207-594-5957; fax: +44-207-225-2716.
E-mail address: renhe.yang@ic.ac.uk (R. Yang).

PII: S0008-8846(00)00493-2

Table 1
Mix proportions

Specimen	Cement:sand:coarse aggregate (by weight)	Water:cement
Mortar cylinder (M)	1:2.5	0.4
Concrete panel (C1)	1:2.28:3.72	0.55
Concrete panel (C2)	1:2.78:4.57	0.70

The effectiveness of the algorithm to separate different types of aggregate in the concrete image is demonstrated.

2. Experimental

A JEOL 5410LV SEM equipped with the Oxford Instruments Imquant image analysis package was employed. The images were collected by a bse detector in low vacuum (9Pa) mode. The accelerating voltage was 20 kV and the spot size was 12. Forty to fifty images were automatically collected for each specimen.

OPC, siliceous sand and dolerite coarse aggregate were used to cast mortar cylinders and concrete panels. Mix proportions are listed in Table 1. Specimens ($40 \times 20 \times 5$ mm) were cut from the concrete panels at 7 days of age and they were dried in an oven at 50°C for 3 days, followed by resin impregnation. The impregnated specimens were ground and polished at grades from 9 μm down to 1/4 μm.

3. Methods

Pores and anhydrous cement particles can be differentiated from the other phases present in a bse image of cement paste by their extreme grey levels. However, the grey levels of aggregate particles in a concrete bse image very often overlap those of the other phases. For example, siliceous aggregate has a similar grey level to that of C–S–H gel as shown in Fig. 1a–c. The hardness of aggregate is generally much higher than that of cement paste and so, polishing may produce aggregate particles with a convex surface resulting in a wider range of grey level than if the surface had been completely flat, causing more overlapping (Fig. 1d–f).

Accordingly, aggregate segmentation by image analysis must be based on characteristics of the phases other than simply grey level. It may be noted from Fig. 1 that the textures of the aggregate particles and the paste matrix are significantly different. The fluctuation of grey level is gentle in the aggregate particles, and in contrast, sharp and frequent in the paste matrix. This can form the basis of an algorithm for aggregate segmentation, using a combination of several image analysis techniques that are available in most modern image analysis software packages. Fig. 2 shows the flow chart of the algorithm.

The concrete image in Fig. 1d is used to demonstrate the procedure of aggregate segmentation. The first operation is

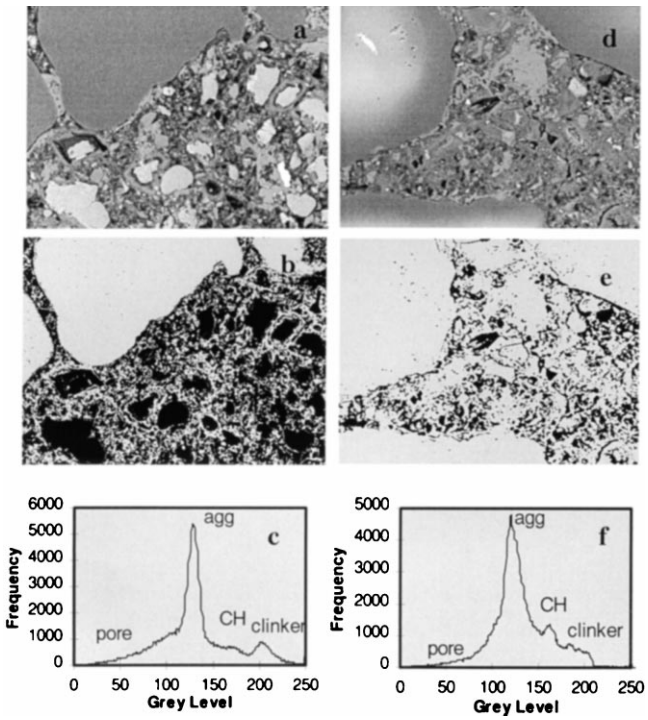

Fig. 1. Aggregate segmentation by grey-level thresholding (specimen C1). (a)+(d) Grey images; (b)+(e) binary images by grey-level thresholding; (c)+(f) histograms for (a) and (d).

edge detection of the aggregate particles by the "gradient" technique. This involves generating an image whose grey levels are defined as the differentials of the grey levels in the grey image. Fig. 3b shows the gradient image of the grey image (Fig. 3a). In the gradient image, the boundaries between the phases are enhanced and turned into high (light) grey levels, whereas the bulks of the phases are turned into low (dark) grey levels. The gradient image is then converted into a binary image by selecting the appropriate grey-level thresholds so as to separate the aggregate particles as far as possible from the paste matrix and, simultaneously, the paste matrix is cut into small pieces. Fig. 3c is a positive binary image of the gradient image after

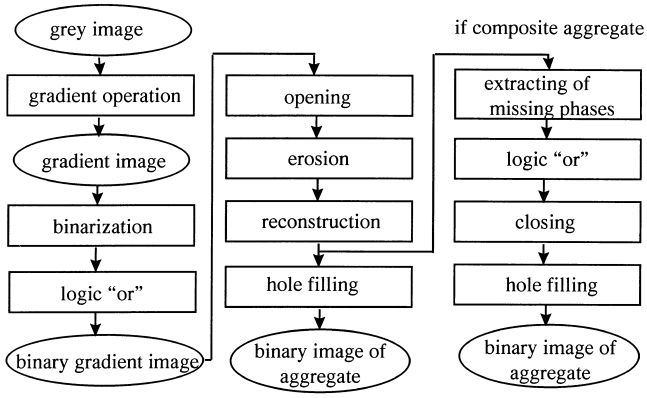

Fig. 2. Flow chart of the algorithm for aggregate segmentation.

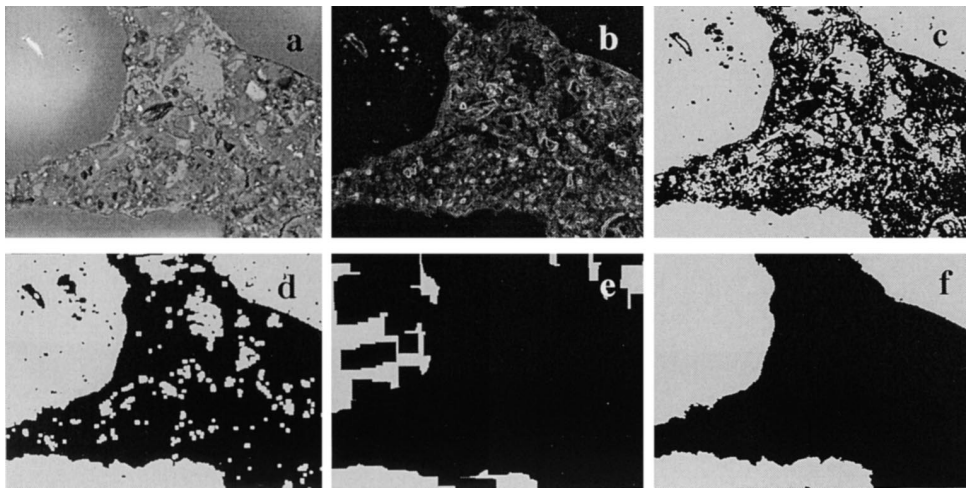

Fig. 3. Aggregate segmentation by combination of grey-level thresholding, filtering and binary operations. (a) Grey image; (b) gradient image; (c) positive binary gradient image; (d) opening; (e) eroding; (f) reconstructing.

grey-level thresholding and subtraction of the pores. It can be seen that the aggregate boundaries in the grey image are generally identified, but some residual fragments of the paste matrix are still included in the image and some of them are attached to aggregate particles by narrow bridges.

Binary operations are required to erase the residual fragments of paste, but retain the aggregate. The "opening" operation is used first to disconnect the paste fragments from the aggregate particles, as shown in Fig. 3d. Opening involves a disk rolling along the inside of the boundary of the object, disconnecting the parts of the object that the disk cannot reach (Fig. 4b). Then the opened image is "eroded." This involves a disk rolling along the boundary of the object eroding a thickness equivalent to the disk radius from the edge of the object (Fig. 4c). Since the residual paste fragments are much smaller than the aggregate particles, the extent of erosion can be set to erase the residual paste fragments completely, but only the surface of the aggregate particles, as shown in Fig. 3e. Finally, the aggregate particles in the eroded image are "reconstructed" by changing the shapes of the objects present in the image into those of the corresponding objects in the reference image (Fig. 4b). The image in Fig. 3c is chosen as the reference image for the reconstruction. Therefore, the reconstruction takes place in the aggregate particles, but not in the residual paste fragments because they are not present in Fig. 3e. After reconstruction and hole-filling operations, a realistic segmentation of the aggregate particles in the grey image (Fig. 3a) is achieved, as presented in Fig. 3f.

With some modifications, the algorithm proposed above can also deal with aggregate having composite grey levels. An example is given in Fig. 5, which shows concrete containing dolerite coarse aggregate. The grey image containing the dolerite aggregate (Fig. 5a) is treated by the algorithm described above without performing the last operation, i.e., hole filling. The result of the binary segmentation of the aggregate particles is presented in Fig. 5b. It is noted that the paste matrix is erased precisely. However the bright phase in the composite aggregate is missing and phase boundaries are present in the composite aggregate particle. Several additional binary operations are required to amend the image in Fig. 5b. The missing bright phase can be extracted from the grey image (Fig. 5a) by grey-level thresholding as shown in Fig. 5c. They are added to the image of Fig. 5b by the logic operation "OR," resulting in

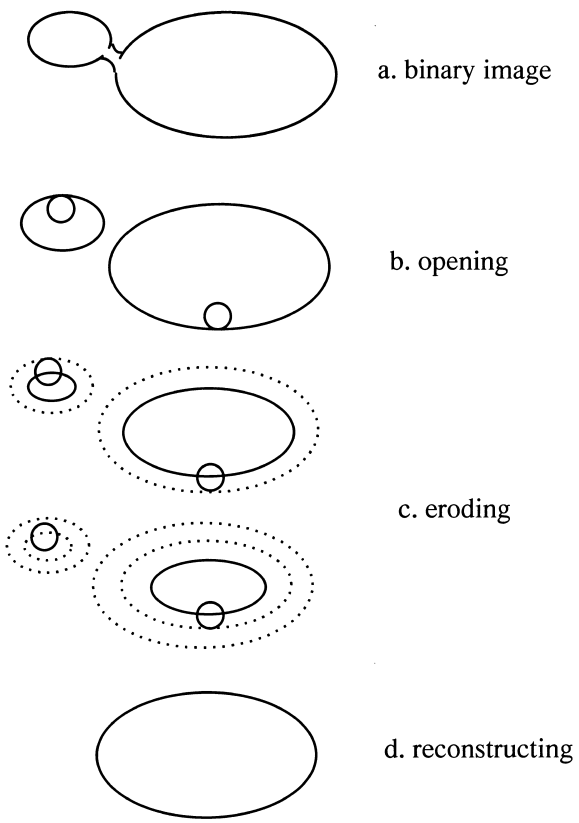

Fig. 4. Sketches of binary operations for aggregate segmentation.

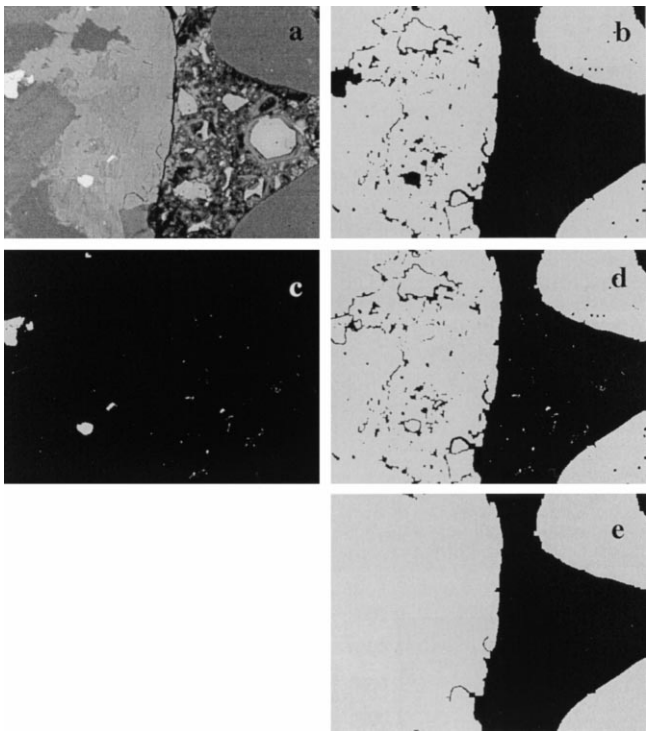

Fig. 5. Composite aggregate segmentation. (a) Grey images; (b) the operations as in Fig. 3; (c) extracting the missing phases by grey-level thresholding; (d) logic "or"; (e) closing and hole filling.

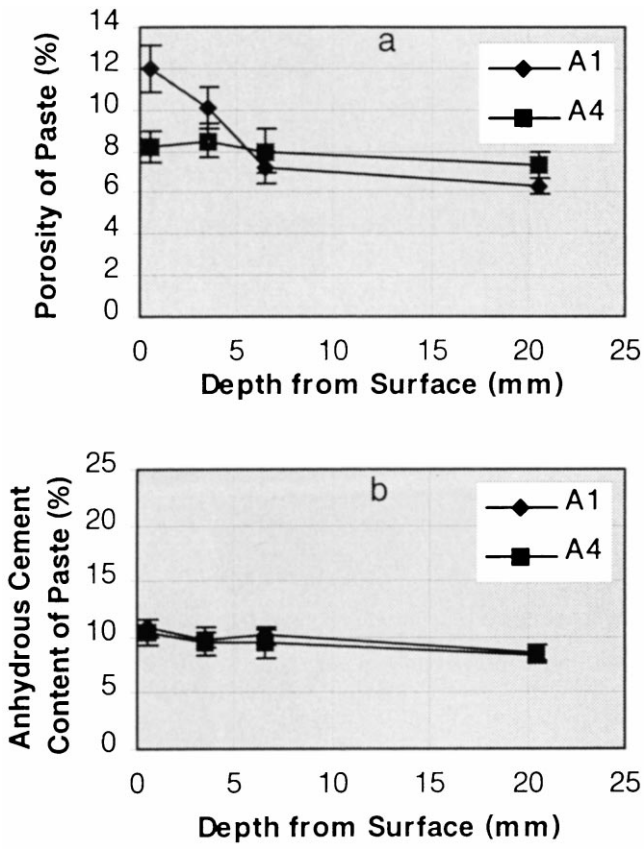

Fig. 6. Porosity (a) and anhydrous cement content (b) with depth in the concrete panels with (A4) and without (A1) wet curing for 7 days.

the image of Fig. 5d. Then the closing operation (the inverse of opening) followed by the hole-filling operation is performed to achieve the ultimate segmentation of the aggregate particles as shown in Fig. 5e.

The algorithm has been written as a computer program attached to the Imquant image analysis system, which can be run semiautomatically to analyze porosity and anhydrous cement content in concrete with segmentation of aggregate. Manual determinations of the grey-level thresholds and the binary parameters are required for precise segmentation of aggregate.

4. Results

The above image analysis method was tested by segmentation of sand particles in laboratory-prepared mortar and concrete specimens. Forty to fifty images at 500 × magnification were taken automatically by SEM for each specimen. The fraction of coarse aggregate in a single −20 × 40 mm concrete SEM specimen is unlikely to be representative of the concrete as a whole due to its relatively large size. In order to avoid testing many SEM specimens, the image taking deliberately avoided the large dolerite aggregate particles and was restricted to the mortar areas of the concrete. The measured sand fractions in the mortar and the mortar parts of the concretes were compared with those calculated on the basis of the mix proportions of the specimens. The specific gravities of OPC and siliceous sand were taken to be 3.15 and 2.62, respectively. The measured and calculated results are compared in Table 2; good agreement is present in all cases.

Table 2
Sand fractions determined by image analysis and calculated on the basis of mix proportions of mortar and concrete

	Fraction of sands in the mortars (volume%)		
Specimen	Calculated	Measured	Relative error (%)
M	57.09	55.28	−3.2
C1	50.07	49.47	−1.2
C2	51.11	49.22	−3.7

There is usually a gradient in aggregate content near the surface of concrete elements. The proposed image analysis method, benefiting from aggregate segmentation, is able to measure profiles of porosity and anhydrous cement content with depth without the complicating influence of aggregate distribution. Effects of curing on the microstructure of the cement paste in concrete are presented in Fig. 6. A concrete panel (C1) with wet curing (wet hessian sealed in polythene) for 7 days (A4) exhibits little variation in cement paste porosity with depth, while the concrete panel stripped at one day and then directly exposed to UK

sheltered outdoor conditions (relative humidity 70–90%) for 7 days (A1) has higher porosity in the surface region. The discrepancy due to curing extends to a depth of about 6 mm from the surface of the concrete. The effect of curing on cement hydration is seen to be negligible; this is not inconsistent with the porosity results, as discussed in Ref. [11].

5. Conclusions

• The rational combination of image analysis techniques (grey-level thresholding, filtering and binary operations) can be used to separate aggregate from cement paste in bse images of concrete.

• With segmentation of aggregate, analysis of bse images can be effectively used to measure microstructural parameters such as the porosity and anhydrous cement content of cement paste in concrete.

References

[1] K.L. Scrivener, H.H. Patel, P.L. Pratt, L.J. Parrott, Analysis of phases in cement paste using backscattered electron images, in: L.J. Struble, P.W. Brown (Eds.), Microstructural Development During Hydration of Cement, Mater. Res. Soc. Symp. Proc. 85 (1987) 67–76.

[2] H. Zhao, D. Darwin, Quantitative backscattered electron analysis for cement paste, Cem. Concr. Res. 22 (1992) 695–706.

[3] K.O. Kjeilsen, R.J. Detwiler, O.E. Gjørv, Backscattered electron image analysis of cement paste specimens: Specimen preparation and analytical methods, Cem. Concr. Res. 21 (1991) 388–390.

[4] D.A. Lange, H.M. Jennings, S.P. Shah, Image analysis techniques for characterization of pore structure of cement based materials, Cem. Concr. Res. 24 (1994) 841–853.

[5] Y. Wang, S. Diamond, An approach to quantitative image analysis for cement pastes, Mater. Res. Soc. Symp. Proc. 370 (1995) 23–32.

[6] D. Darwin, M.N. Abou-Zeid, Application of automated image analysis to the study of cement paste microstructure, Mat. Res. Soc. Symp. Proc. 370 (1995) 3–12.

[7] S. Diamond, M.E. Leeman, Pore size distributions in hardened cement paste by SEM image analysis, Mater. Res. Soc. Symp. Proc. 370 (1995) 217–226.

[8] M. Barrioulet, R. Saada, E. Ringot, A quantitative structural study of fresh cement paste by image analysis: Part 1. Image processing, Cem. Concr. Res. 21 (1991) 835–843.

[9] K.L. Scrivener, E.M. Gartner, Microstructural gradients in cement paste around aggregate in particles, Bonding in Cementitious Composites, S. Mindess, S.P. Shah (Eds.), Mater. Res. Soc. Symp. Proc., Pittsburgh vol. 114 (1988) 77–86.

[10] A.M. Werner, D.A. Lange, Quantitative image analysis of masonry mortar microstructure, J. Comput Civil Eng. 13 (1999) 110–115.

[11] N.R. Buenfeld, R. Yang, On-site curing of concrete — microstructure and durability. Funders Report/CP/63, CIRIA, 2000.